Contrasting Conditions of Surface Water Balance in Wet Years and Dry Years as a Possible Land Surface–Atmosphere Feedback Mechanism in the West African Sahel

A. R. LARE AND S. E. NICHOLSON

Department of Meteorology, The Florida State University, Tallahassee, Florida

(Manuscript received 18 February 1992, in final form 10 August 1992)

ABSTRACT

The climate of West Africa, in particular the Sahel, is characterized by multiyear persistence of anomalously wet or dry conditions. Its Southern Hemisphere counterpart, the Kalahari, lacks the persistence that is evident in the Sahel even though both regions are subject to similar large-scale forcing. It has been suggested that land surface–atmosphere feedback contributes to this persistence and to the severity of drought. In this study, surface energy and water balance are quantified for nine stations along a latitudinal transect that extends from the Sahara to the Guinea coast. In the wetter regions of West Africa, the difference between wet and dry years is primarily reflected in the magnitude of runoff. For the Sahel and drier locations, evapotranspiration and soil moisture are more sensitive to rainfall anomalies. The increase in evapotranspiration, and hence latent heating, over the Sahel in wet years alters the thermal structure and gradients of the overlying atmosphere and thus the strength of the African easterly jet (AEJ) at 700 mb. The difference between dry and wet Augusts corresponds to a decrease in magnitude of the AEJ at 15°N on the order of 2.6 m s^{-1}, which is consistent with previous studies of observed winds.

Spatial patterns were also developed for surface water balance parameters for both West Africa and southern Africa. Over southern Africa, the patterns are not as spatially homogeneous as those over West Africa and are lower in magnitude, thus supporting the suggestion that the persistence of rainfall anomalies in the Sahel might be due, at least in part, to land–atmosphere feedback, and that the absence of such persistence in the Kalahari is a consequence of less significant changes in surface water and energy balance.

1. Introduction

During the past decade, the African continent has been anomalously dry (Fig. 1). Two of the most severely affected regions are the semiarid Sahel of West Africa and its Southern Hemisphere counterpart, the Kalahari. The rainfall fluctuations in both regions are correlated on the scale of decades and, somewhat less so, for individual years. One notable difference is apparent, however, in the year-to-year persistence of the anomalous rainfall. In the Sahel, the duration of dry or wet episodes is on the order of one or two decades. Rainfall has not exceeded the mean since 1969 (Fig. 2). In contrast, rainfall exceeded the mean in every year from 1950 to 1959. Although on the average rainfall has been abnormally low in the Kalahari during most of the same period and anomalously high in the 1950s, the remarkable persistence so readily apparent in the Sahel series is lacking in the Kalahari. In the latter region, no sequence of "wet" or "dry" years is longer than 4 or 5 years.

We are hypothesizing that the persistence in the Sahel is a manifestation of land–atmosphere feedback, invoked by the changes of surface energy balance induced by anomalously high or low rainfall. A corollary to this hypothesis is that drought or wet years are triggered by large-scale factors in the general atmospheric circulation and/or over the global oceans, acting synchronously in the Sahel and the Kalahari. According to this scenario, the land surface changes induced by the anomalous rainfall (e.g., vegetation, albedo, temperature, soil moisture) would reinforce the atmospheric conditions that produced the anomaly in the Sahel. This would prolong and intensify drought or wet conditions. The absence of such interannual persistence in the Kalahari would then suggest that either the land surface changes are too small in magnitude or spatial extent to have significant feedback on the overlying atmosphere or that the systems that produce rainfall in southern Africa are relatively insensitive to land surface characteristics and processes.

In this study, we examine this hypothesis by assessing the surface water balance for wet years and dry years for representative stations in both regions. The climatonomy model developed by Lettau (e.g., Lettau 1969; Lettau and Baradas 1973) is used to calculate soil moisture, evapotranspiration, and runoff for the mean conditions of the 10 wettest and 10 driest years at each station. The model is forced by precipitation and incoming solar radiation at the top of the atmosphere. The model is then adapted to produce mean

Corresponding author address: Dr. Andrew R. Lare, Applied Research Corporation, NASA GSFC (Code 913), Greenbelt, MD 20771.

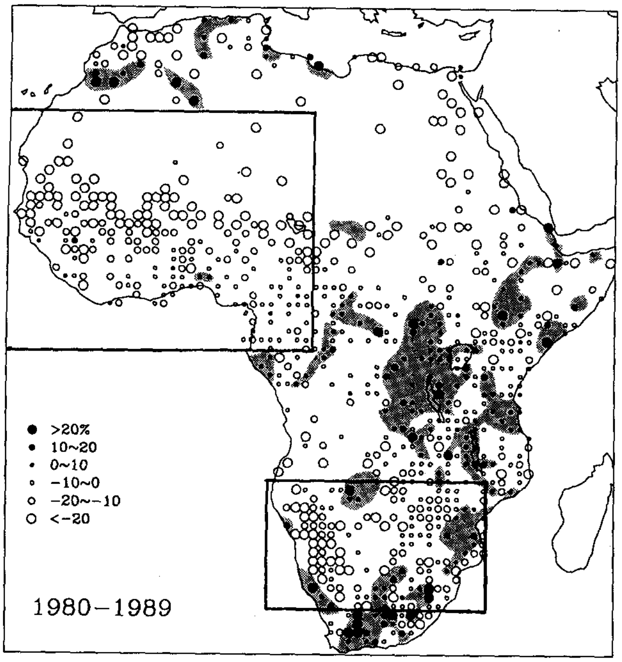

FIG. 1. Mean rainfall for the decade 1980–89 expressed as a percent departure from the long-term mean (i.e., the mean for the entire length of record, commencing in 1901 or as soon thereafter as rainfall observations begin). Station data are averaged over 1° squares to facilitate presentation. Boxed areas indicate regions of interest in this study.

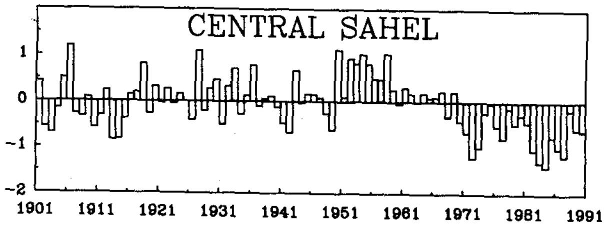

FIG. 2. Rainfall fluctuations in the West African Sahel (1901 to 1990) expressed as a regionally averaged standardized departure (departure from the mean divided by the standard departure).

spatial fields of the relevant variables for the 10 wettest and 10 driest years in both regions. The modifications, described in section 2d, facilitate data input for a large number of stations.

The stations and analysis regions are shown in Fig. 3, together with isohyets of mean annual rainfall. The nine Sahelian stations (Fig. 3a) were chosen to represent the north–south rainfall gradient from the Sahara to the Guinea Coast. They run roughly along a northeast–southwest transect, which shifts abruptly to the west at about 8°N, in order to bypass the anomalous dry zone (Trewartha 1961) of southern Ghana. Six Kalahari stations (Fig. 3b) were chosen to typify a range of conditions. The range is smaller than in the Sahel, however, because in selecting appropriate stations, we limited choices to regions that exhibit significant contrast in rainfall between the 10 wettest and 10 driest years for the Kalahari as a whole.

2. The climatonomy model

a. Overview

The model used in this study is an adaptation of the Lettau three-part "climatonomy" model that was developed in the late 1960s (Lettau 1969; Lettau and Lettau 1969, 1975). Climatonomy was conceived as a regional-scale model of surface energy and water balance, and it has been applied to a number of geographic locations. Recently, the climatonomy model has been used to study surface water balance in the Great Plains (Pinker and Corio 1987; Corio and Pinker 1987), the West African Sahel (Nicholson and Lare 1990), and areas of the United States (Lettau and Hopkins 1991).

The accuracy of climatonomic model output has been verified in a number of experiments. Lettau (1969) applied the model to several areas in North America using observed data encompassing several

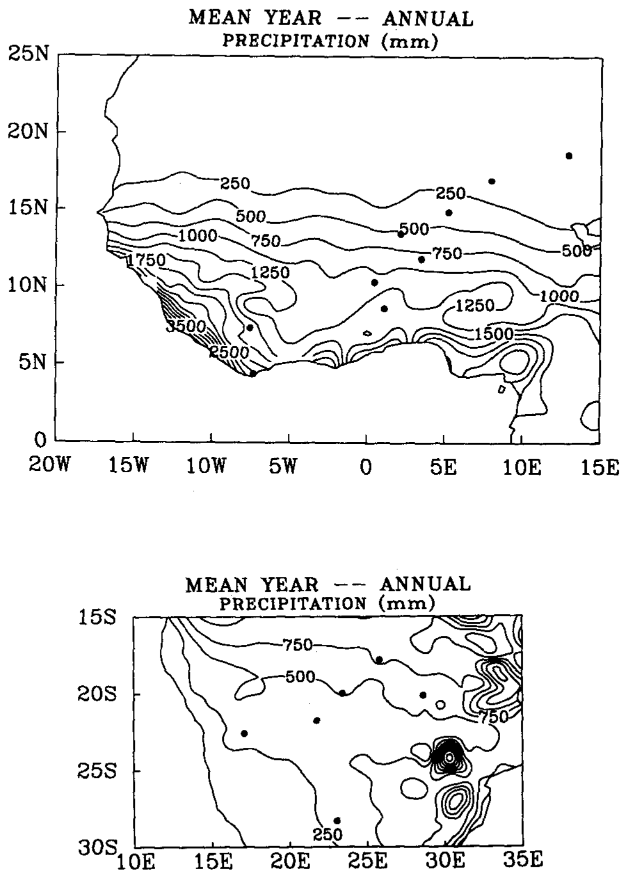

FIG. 3. Map of stations used in the study and isohyets of mean annual rainfall, in mm: (a) West Africa, (b) the Kalahari and surrounding regions.

years and found general agreement between monthly observed and calculated runoff, evapotranspiration, and soil moisture values. Lettau and Baradas (1973) applied the model to the Mabacan River watershed in the Philippines for a 12-yr period. Annual averages of observed runoff were found to be correlated at the 0.89 level with calculations, and monthly evapotranspiration calculations also compared well with empirical data for the region. Corio and Pinker (1987) tested the validity of the model on shorter temporal and smaller spatial scales than the climatic scales associated with previous studies, conducting an experiment for the state of Kansas as well as for several smaller individual watersheds. Calculated runoff compared well with observed values when the entire state was considered, resulting in phase differences of less than 1 month and similar amplitudes. Nicholson and Lare (1990) found good agreement with observed soil moisture and other parameters in the Sahel.

The model consists of three subunits: shortwave radiation climatonomy, evapoclimatonomy, and thermoclimatonomy (Lettau 1969; Lettau and Lettau 1969, 1975). The shortwave radiation submodel is used to calculate ground-absorbed solar radiation from incoming solar radiation (Lettau and Lettau 1969; Lare and Nicholson 1990). Absorbed solar radiation in combination with rainfall forces the evapoclimatonomy submodel, which in turn predicts monthly mean evapotranspiration (E), runoff (N), and soil moisture (m). Precipitation, evapotranspiration and ground-absorbed radiation provide input to the third submodel.

In this study, only the evapoclimatonomy submodel is used. However, its input includes ground-absorbed solar radiation, which was calculated with the shortwave submodel. The evapoclimatonomy submodel is described in section 2c, while details of the shortwave model are summarized in section 2b and presented in Lare and Nicholson (1990). The shortwave model results for the locations described in this article will appear in a sequel concerned with surface energy balance.

b. Shortwave radiation climatonomy

In the shortwave radiation submodel, extraatmospheric irradiance is used as the forcing function. Five governing equations partition the incoming solar radiation into basic energy balance components and provide a description of the physical relationships between them. The five equations for clear skies relate to absorption by the atmosphere H^*, planetary albedo A^*, diffuse radiation d^*, and ground absorption $(1 - a_s)G^*$ where a_s is surface albedo and G^* is global radiation:

$$1 - A^* = H^* + (1 - a_s)G^* \tag{1}$$

$$1 - G + d^* = \alpha + \sigma \tag{2}$$

$$A^* = \mu\sigma + (1 - \alpha)a_s G^*(1 - \kappa\sigma) \tag{3}$$

$$d^* = (1 - \mu)\sigma + (1 - \alpha)a_s G^* \kappa\sigma \tag{4}$$

$$H^* = \alpha(1 + a_s G^*). \tag{5}$$

The parameters α and σ denote that part of the solar beam which is absorbed and scattered, respectively, while μ and κ represent the fraction of radiation that is effectively scattered back to space and the backscattering of ground-reflected radiation. Contributions by clouds are assumed to be additive for absorption processes and distributive for scattering processes. A more complete discussion of the governing equations and necessary parameterizations may be found in Lettau and Lettau (1969) and Lare and Nicholson (1990).

c. Evapoclimatonomy

The evapoclimatonomy submodel is in essence a numerical solution to the integration of the basic hydrologic balance equation

$$P = E + N + dm/dt, \tag{6}$$

where P is rainfall, E is evapotranspiration, N is runoff, and dm/dt is the change in soil moisture storage. Three basic assumptions, which are paramount to the model's simplicity, are described below. The original model appeared in Lettau (1969).

The basic premise of the model is as follows:

1) For a stationary climate the long-term mean of dm/dt is zero, that is, there is no net change in soil moisture storage. Thus

$$\bar{P} = \bar{E} + \bar{N}. \tag{7}$$

In general, this assumption is most valid for the larger regions and the longer time periods.

2) Evapotranspiration and runoff can both be partitioned into immediate and delayed processes:

$$E = E' + E'' \tag{8}$$

$$N = N' + N'', \tag{9}$$

where the single primes denote "immediate" processes occurring in the same month as the rainfall and the double primes denote runoff and evaporation of rain that fell in previous months. The physical rationale for assumption 2 is the need to distinguish between the time variations of E and N coupled with concurrent precipitation and those supplied by subsurface moisture, which is dependent on rainfall from previous months.

3) The delayed processes of runoff N'' and evapotranspiration E'' vary directly with soil moisture m such that

$$N''(t) = \overline{N''}m(t)/\bar{m} \tag{10}$$

$$E''(t) = \overline{E''}m(t)/\bar{m}. \tag{11}$$

Equations (8) and (9) allow for the definition of a quantity called "reduced precipitation" (P'), which represents the amount of the mass input that is not lost by surficial processes of immediate runoff and evapotranspiration and thus is available for soil moisture storage. Therefore,

$$P' = P - N' - E'. \quad (12)$$

In view of the preceding discussion, the soil moisture storage term is reduced to

$$dm/dt = P' - (N'' + E''). \quad (13)$$

The above equation (13) is solved using two empirical concepts, "evaporivity" e^* and "residence time" t^*, which are subsequently defined and used to partition the immediate and delayed processes.

The sum of equations (10) and (11) yields an equation that defines a new characteristic dimensional parameter:

$$N'' + E'' = (\overline{N''} + \overline{E''})m/\bar{m} = m/t^*, \quad (14)$$

where $t^* = \bar{m}/(N'' + E')$ denotes a time interval most conveniently expressed in months. Physically, t^* can be interpreted as a "residence time" or "turnover period" that is characteristic of a basin and signifies the time required for a volume of water equal to the annual mean of exchangeable soil moisture to be depleted by the "delayed" processes of runoff and evapotranspiration. The actual value of t^* is a function of soil type and the potential evapotranspiration rate (PET), with higher PET values resulting in lower residence times. Residence time (Table 1) is calculated after Serafini and Sud (1987) as a function of PET, the wilting point (m_{wp}, the point at which the vegetation cannot absorb enough moisture to sustain itself and begins to wilt), and field capacity (m_{fc}), so that

$$t^* = \frac{\gamma}{\lambda \mathrm{PET}} \ln \frac{e^{\lambda m_{fc-1}}}{e^{\lambda m_{wp-1}}}, \quad (15)$$

where

$$\lambda = \frac{\alpha_v}{m_{fc} - m_{wp}} \quad (16)$$

and

$$\gamma = 1 - e^{-\alpha_v}. \quad (17)$$

In the above equation, α_v accounts for variations in vegetation type. According to Serafini and Sud (1987), α_v may have a value from 16 to 20 for forest vegetation types, while a value of 2 may be more appropriate for desert vegetation. Mintz and Serafini (1984) suggested using $\alpha_v = 6.81$ to cover most vegetation types. Wilting point and field capacity are determined after Saxton et al. (1986) as a function of soil type (i.e., percent sand and clay content). Finally, PET is taken from FAO (1984) and determined using a modified version of the Penman formula.

The parameterization of immediate processes is likewise achieved using proportionalities based on the annual balance equations. For immediate evapotranspiration (E'), Lettau (1969) defined an additional characteristic parameter (e^*), termed the "evaporivity," which is applied in the following equations:

$$E'(t) = e^* \cdot P(1 - a_s)G^*/\overline{(1 - a_s)G^*} \quad (18)$$

$$\overline{E'} = \overline{e^* \cdot P}. \quad (19)$$

In the above, $(1 - a_s)G^*$ and $\overline{(1 - a_s)G^*}$ are the monthly and annual "forcing functions," that is, energy input via absorbed solar radiation. Thus, e^* is a nondimensional measure of the capacity of the land surface to use a portion of the monthly solar radiation to evaporate precipitation received during the same month. Tentative evaluations by Lettau (1971) and others have suggested that e^* will normally be between 0.2 and 0.8. Lettau chose a value of 0.7 for New Delhi, a semiarid subtropical climate with summer rainfall, comparable to most of our study sites.

In the study of the central Sahel by Nicholson and Lare (1990), calculations were simplified by assuming $N' = 0$, which is generally the case in semiarid regions (Eagleson and Segarra 1985). In order to more accurately treat immediate runoff, an approach originally proposed by Milly and Eagleson (1982) and adapted by Warrilow (1986) has been used in the current study. In essence, immediate runoff (Table 1) is a function of mean monthly rainfall rate, mean monthly infiltration rate, and a proportionality constant based on the average fractional area of a grid or region in which precipitation occurs, such that

$$N' = Pe^{-\alpha F/P}. \quad (20)$$

Furthermore, immediate runoff calculations are treated like observations, and therefore, represent a loss of effective rainfall input into the model. Rainfall rate is

TABLE 1. Mean annual precipitation (P), range of soil moisture residence times, and immediate runoff for West African and southern African base stations used in this study.

Station	P (mm)	t^* (months)	N' (mm)
West Africa			
Bilma	17	0.9–1.5	0
Agadez	145	0.8–1.4	46
Tahoua	384	0.4–0.7	6
Niamey	559	0.5–0.9	19
Gaya	834	1.2–2.0	127
Mango	1084	1.5–2.1	312
Sokode	1375	1.8–2.7	486
Man	1702	1.6–2.2	769
Tabou	2318	1.7–2.4	1234
Southern Africa			
Windoek	327	1.4–4.2	56
Postmasburg	333	0.6–2.9	1
Ghanzi	429	0.7–2.8	3
Maun	473	1.1–3.2	0
Bulawayo	597	0.7–1.7	8
Livingstone	739	1.7–4.2	10

determined using hourly synoptic observations and daily precipitation records. Infiltration rate, assumed invariant (Warrilow 1986), is represented as a function of the hydraulic conductivity. Hydraulic conductivity is determined by soil moisture content (immediate top soil surface is assumed to be saturated while infiltration occurs), and by soil type (i.e., sand and clay content) following Saxton et al. (1986). This rate, which is for bare ground, is modified by vegetation density and structure and ground cover as in Rawls et al. (1989), Rawls and Brakensiek (1989), and Wilcox et al. (1990). In general, infiltration rates are higher for soils with high sand content and lower for clay soils. They are also higher for soils where vegetation canopy, ground cover, surface rocks, or leaf litter are present (Gifford 1984). Finally, the proportionality constant α is assumed to be 0.66 for convective rainfall after Eagleson et al. (1987).

Runoff is calculated as a function of the gravitational drainage of existing soil water and the surface runoff due to precipitation exceeding infiltration rate (Warrilow 1986). The annual mean delayed runoff N'' is determined using Saxton et al. (1986). In doing so, it is assumed that there is a single layer of soil with spatially homogeneous soil moisture; that is, horizontal movements of water are neglected. Gravitational drainage varies with soil type, with larger values for coarser soils and smaller ones for fine-grained soils. It also increases with increasing soil moisture. Surface runoff is calculated as a function of the surface infiltration rate and is affected by the spatial variability of rainfall. The use of a proportionality constant accounts for the fact that although the entire region may experience total rainfall that is below the threshold for runoff, a certain percentage of the area may receive amounts great enough to produce runoff in individual locations.

The concepts described above transform the basic budget equation (6) into

$$P - E' - N' = E'' + N'' + dm/dt \qquad (21)$$

$$= m/t^* + dm/dt. \qquad (22)$$

Subtracting the annual average of all terms from the above equation (22) yields

$$p'(t) = (m - \bar{m})/t^* + d(m - \bar{m})/dt, \qquad (23)$$

where p' stands for the time series $P - E' - N' - \overline{(P - E' - N')}$. The ordinary differential equation is solved by

$$m - \bar{m} = e^{-t/t^*}\left[\text{const} + \int e^{t/t^*}p'dt\right], \qquad (24)$$

where "const" denotes an integration constant that is determined by the requirement that the bracketed value (i.e., the annual mean) of the right side must vanish for a stable climate. This equation is solved using stepwise integration, starting with an assumed initial value (m_1) of soil moisture. In a stable climate, the value for the 13th month (m_{13}) must equal m_1. The procedure is iterated until reasonable agreement occurs, that is, until $(m_{13} - m_1) < 0.005$ mm. Usually only two or three iterations are necessary.

d. Adaptations for deriving spatial fields

Derivation of spatial patterns of the surface water balance parameters requires more detail than that provided by the nine West African and the six southern African base stations in the analyses thus far described. To produce the spatial fields, additional stations were selected from the rainfall archive. Each was grouped with the base station most climatically similar to it. Ancillary data for the appropriate base station were then used for each station in the group. However, local information on rainfall, vegetation, and soil type was utilized for each station in the network; thus permitting reasonable approximation of spatial fields for wet and dry years, while keeping the required additional data input to a minimum. Thus, the model was run for each station using input for the appropriate base station together with the precipitation, soil type, and vegetation type at the station itself.

3. Data and climatic background

a. General climatology

This study focuses on the semiarid Sahel and Kalahari regions of Africa, and regions in geographical proximity. The Sahel has been defined in numerous ways in the literature. In the strictest sense, it is the latitudinal belt south of the Sahara, composed of savanna vegetation and with rainfall ranging from about 100 mm yr^{-1} in the north to about 400 mm yr^{-1} in the south. Here, the term "Sahel" is loosely used to denote the whole semiarid zone south of the Sahara to a latitude of roughly 12°–13°N. Mean annual rainfall ranges from about 500 mm yr^{-1} in the north to 1200 mm yr^{-1} in the south (Fig. 3a). In this region, the rainy season, which is limited to the summer or "high-sun" season, becomes increasingly shorter with increasing latitude, ranging from about 1 to 5 months. In the Kalahari, the rains likewise occur in the high-sun season and last about 5 to 6 months. In most areas, mean annual rainfall (Fig. 3b) is on the order of 250 to 600 mm yr^{-1}. Rainfall is well distributed over the season, but strongly concentrated in the two or three wettest months in the Sahel. Hence, peak monthly intensity is greater over the Sahel, 200 to 300 mm mo^{-1}, compared to 100 to 200 mm mo^{-1} at most Kalahari stations.

There are two other major climatic differences between the Sahel and Kalahari. First, as a consequence of the Kalahari's higher latitude, its radiation regime is more typical of the midlatitudes than the tropics, with a more pronounced annual march. This has implications for the water balance. Also in contrast to the Sahel, the rain-bearing disturbances of the Kalahari are to some extent tropical/extratropical hybrids. As a result, some rains are nearly frontal in nature, thus being longer in duration and lower in intensity than those generally associated with tropical systems. This likewise affects the runoff and evaporation, and, hence, surface water balance.

b. *Forcing functions of the model*

The patterns of climate described above are illustrated in Fig. 4, which shows the major forcing functions of the model: solar irradiance (the shortwave model), ground-absorbed solar radiation, and precipitation (evapoclimatonomy). Extra-atmospheric solar radiation is calculated from standard formulas (Sellers 1965) using Fourier series–type expressions for eccentricity and the solar declination after Spencer (1971). Ground-absorbed solar radiation is calculated using the shortwave submodel, as described fully in Lare and Nicholson (1990). The rainfall data derive from a continental archive described in Nicholson (1986).

Significant contrast is apparent between the Sahel and the Kalahari. The increasing intensity and duration of the Sahel rainy season from north to south (Fig. 4a) is clearly evident, as is the change to a bimodal seasonal distribution south of the Sahel (i.e., at Tabor, circa 10°N). The peak intensity reaches at least 200 mm mo^{-1} in all but the driest stations. In the Kalahari, high rainfall is maintained for a longer period, but it barely exceeds 100 mm $month^{-1}$ at any but the wettest station. In the Sahel, the portion of the extraatmospheric solar insolation which is ultimately absorbed by the ground is somewhat smaller than in the Kalahari (Fig. 4b). In many Sahelian stations, ground-absorbed radiation actually reaches a minimum during the rainy season, as a result of cloud cover, and is somewhat lower than the amount received in the Kalahari during the rainy season. In the Kalahari, ground-absorbed radiation reaches a maximum during the rainy season.

c. *Ancillary data*

The input data required for model parameterizations in the shortwave model include atmospheric constituents, aerosols, cloud cover, and surface albedo (Table 2). Water vapor was obtained from FAO (1984); ozone, carbon dioxide, and oxygen were derived from standard sources (Sasamori et al. 1972; Lacis and Hansen 1974; London et al. 1976). Rayleigh scattering (Bird and Hulstrom 1981) was calculated from relative optical air mass, after Rodgers (1967). Monthly mean cloud cover was obtained from Warren et al. (1986). Although significant errors in ground-absorbed solar radiation, on the order of 3% to 9% in the dry season and 10% to 19% during the wet season (Lare and Nicholson 1990), occur as a result of a ±20% error in cloud amount, the effect of these errors on the evapoclimatonomy submodel is primarily manifested as a modulation in the amplitude of the annual cycle (Nicholson and Lare 1990). Surface albedo was taken from global monthly fields derived by Dorman and Sellers (1989) on the basis of vegetation type. Although the grid for these is coarse, 4° × 5°, sensitivity studies run in the model indicate that albedo errors as large as 50% resulted in soil moisture differences of less than 9% (Nicholson and Lare 1990). Aerosols were very roughly estimated based on regressions relating rainfall, visibility, and turbidity.

Input data required for the evapoclimatonomy submodel include vegetation cover, soil texture, potential evapotranspiration (PET), and evaporivity e^*. Vegetation cover was derived from Dorman and Sellers (1989), soil texture from FAO/UNESCO (1977), and PET from FAO (1984). Evaporivity was the most difficult parameter to quantify. Tentative evaluations by Lettau (1971) and others have suggested it will normally lie between 0.2 and 0.8, with 0.7 being typical of a semiarid subtropical climate with summer rainfall. The values used here were determined empirically, using results of previous studies (Lettau 1971; Pinker and Corio 1987; Nicholson and Lare 1990).

4. Model results

The model is initially run for each of the stations shown in Fig. 2. The input variables are assumed to be representative of long-term (i.e., multiyear) means. The only highly variable input parameter is rainfall, and the mean values used in the model are averaged over the entire length of record at each station. In nearly all cases, the period of record is from 1921 to 1984 or longer. Thus, the model results represent averages for an approximately 60-yr period. On this time scale, the assumption of a stable climate ($dm/dt = 0$) is quite reasonable.

Once the mean model output is derived, the model is rerun for each station, using as input for the "wet" case the monthly mean rainfall averaged for the 10 wettest years at each station and for the dry case, the mean for the 10 driest years. Other input parameters, such as cloud cover and aerosols, remain unchanged. Next, the model is adapted to derive spatial fields of the major output variables: ET, soil moisture, and runoff. Simplifications incorporated in the model to facilitate this are described in section 2d.

The assumption of no systematic changes of cloud cover from dry to wet years was found to be true for Niamey, a typical Sahelian station. This is due to the fact that not all disturbance lines that traverse the region are rain bearing; some are accompanied by nothing more than an increase in cloudiness. Furthermore, the difference between a wet year and a dry year is primarily due to the occurrence, or lack thereof, of as few as one or two intense rainfall events. The assumption of invariant aerosols is unrealistic, but inconsequential because aerosols have very little effect on the results of the evapoclimatonomy submodel in rainfall-limited, semiarid environments (Nicholson and Lare 1990).

a. *Water balance for typical wet and dry years at individual stations*

Figure 5 shows the results of the wet and dry cases for Sahelian stations. Mean rainfall for each period is given for each station, together with model-calculated soil moisture, evapotranspiration, and runoff. Except for the two southernmost stations, the reduction in rainfall in the dry years is essentially limited to the two or three wettest months (July to September). This is true even for stations with a considerably longer rainy season. At the coast (Tabou), where two rainy seasons are apparent, the later rainy season is most affected during the dry years. This includes the months of August and September, which is also when rainfall is reduced at Sahelian stations during the dry years. At the three stations most comparable to the Kalahari (Tahoua, Niamey, and Gaya), maximum monthly rainfall drops from about 200 to 300 mm in the wet years to about 100 to 150 mm during the dry years. From Agadez to Mango, maximum rainfall occurs in August in both dry and wet years.

At the northernmost stations, these changes are reflected primarily in evapotranspiration (ET) and soil moisture. Evapotranspiration reaches about 100 to 150 mm mo^{-1} in the rainy season during wet years (except at Bilma) and soil moisture at the same time is on the order of 75 to 200 mm. Both are reduced in the wet season by about 50% in the dry years. The changes, as with rainfall, are most apparent from July to September. Soil moisture tends to peak about 1 month after rainfall in both dry and wet years, while ET peaks in the same month as rainfall. It must be noted that the soil moistures depicted in Fig. 5 represent the sum of soil moisture available for evaporative processes and that unavailable due to strong adhesive forces (i.e., residual water content). For example, even though soil moistures at Bilma are higher than those at some wetter climates farther south, almost all of the soil moisture is residual and thus unavailable for evaporative processes. Residual water content is determined after Rawls and Brakensiek (1989) as a function of percent organic matter content, percent clay content, and cation exchange capacity; all of which are taken from FAO/UNESCO (1977).

An interesting change occurs at Gaya, where mean annual rainfall is 829 mm. There, the change in ET and soil moisture from wet to dry years is considerably smaller than farther north; south of Gaya they are virtually invariant. Instead, rainfall changes are manifested primarily in runoff. Also, from Gaya southward both ET and soil moisture tend to peak 1 month after rainfall. Another interesting change is apparent in going southward in wet years: rainy season ET begins to decrease because of increasing runoff. Maximum monthly values occur between about 12°N and 15°N (Gaya to Tahoua). During dry years, the maximum lies near Mango and Sokode, about 9°N to 10°N.

The contrast between wet and dry years at the Kalahari stations is considerably different. First of all, rainfall is significantly reduced in dry years in 5 to 6 months (compared to 2 or 3 in the Sahel). Also, the month of maximum rainfall tends to shift from January in wet years to December or February in dry years. As in West Africa, monthly rainfall is about 50% lower during dry years.

Changes of ET and soil moisture are likewise apparent in all months of the rainy season. At all six stations, ET reaches about 75 to 100 mm mo^{-1} during wet years; soil moisture, about 50 to 150 mm, except at Livingstone, where it reaches about 400 mm in the wettest months. Both are reduced by roughly 50% during dry years. In general, ET and soil moisture are higher in the Sahel than in the Kalahari. The annual march of ET parallels that of rainfall, but soil moisture tends to peak 2 to 3 months after rainfall at drier stations, 1 to 2 months later at wetter stations. The timing of maximum soil moisture shifts only slightly during the drier years. In general, runoff is low at the Kalahari stations and is close to zero at all of them during dry years. Large changes of runoff occur primarily at the two wettest stations, Bulawayo and Livingstone. Presumably, this would be different if wetter stations farther north were examined.

b. *Spatial patterns of hydrologic variables in dry and wet years*

Figure 6a shows the difference between the ten wettest and ten driest years in the Sahel. Values are given for August, the wettest month, for rainfall, soil moisture, evapotranspiration, and runoff. In interpreting the results, it must be kept in mind that the difference fields are related not only to the precipitation differences in August, but also to those of previous months. In much of the Sahel the contrast in rainfall exceeds 100 mm mo^{-1}, but to the south rainfall differences are small or negative. The corresponding changes of soil moisture are in excess of 20 mm for a large zone extending from about 12°N to 18°N. A large difference in evapotranspiration is evident over a greater area: in excess of 20 mm mo^{-1} in a zone roughly extending from about 13°N to 20°N, in excess of 50 mm mo^{-1} throughout most of the area between 14°N and 18°N. Since differences of the opposite sign prevail north and south of about 10°N, there is a strong change of the meridional gradient of soil moisture and ET between wet and dry years. The contrast in runoff between wet years and dry years is on the order of 50 to 100 mm mo^{-1} throughout much of the Sahel from about 10°N to 15°N. Further south, runoff is reduced, by over 50 mm mo^{-1} in some areas.

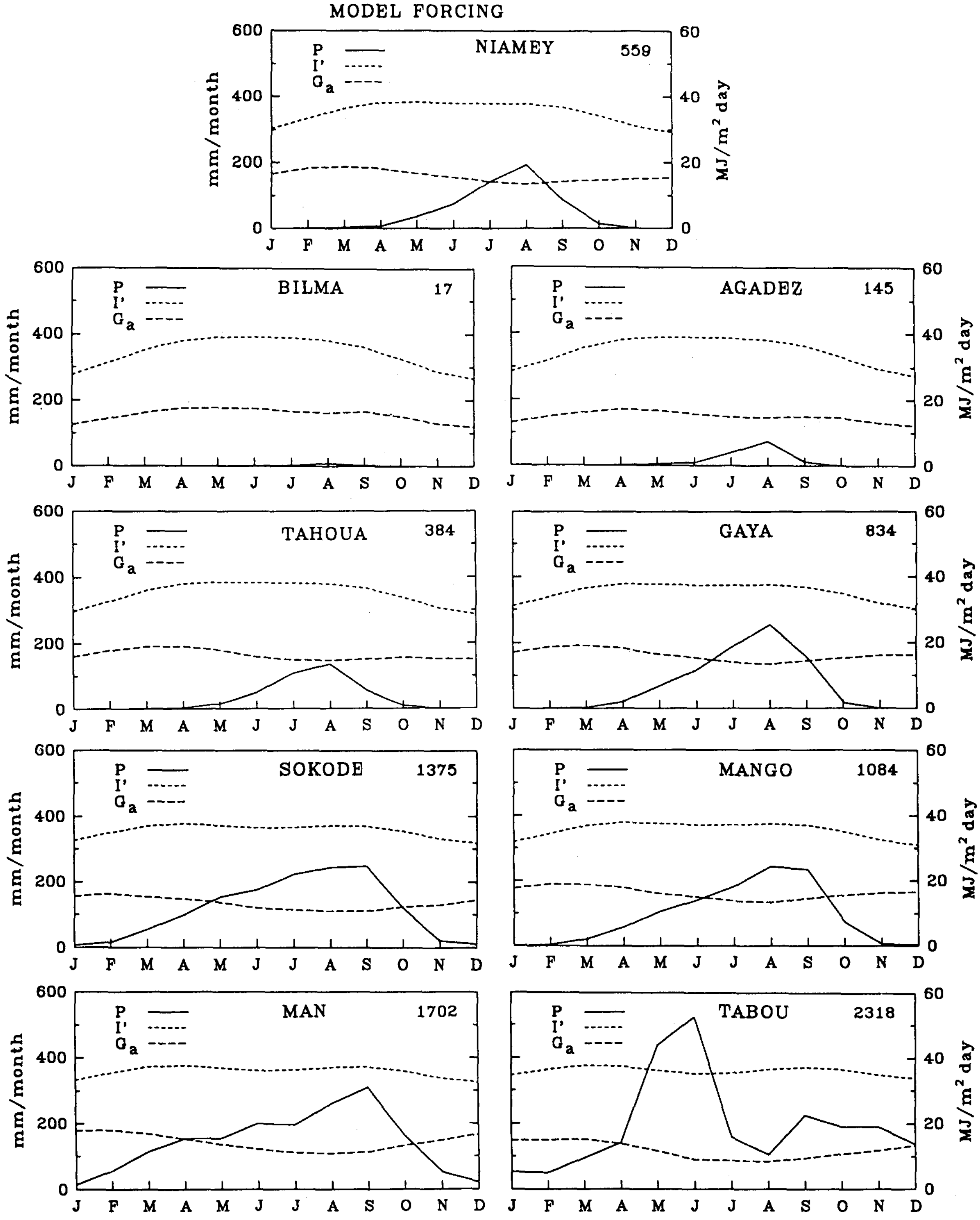

FIG. 4. Seasonal march of model forcing functions: solar irradiance I', ground-absorbed radiation G_a, and monthly precipitation P; mean annual rainfall is in upper right. (a) A typical central Sahel station (Niamey) and other West African stations along the north–south transect in Fig. 3a. (b) Stations in the Kalahari and surrounding regions.

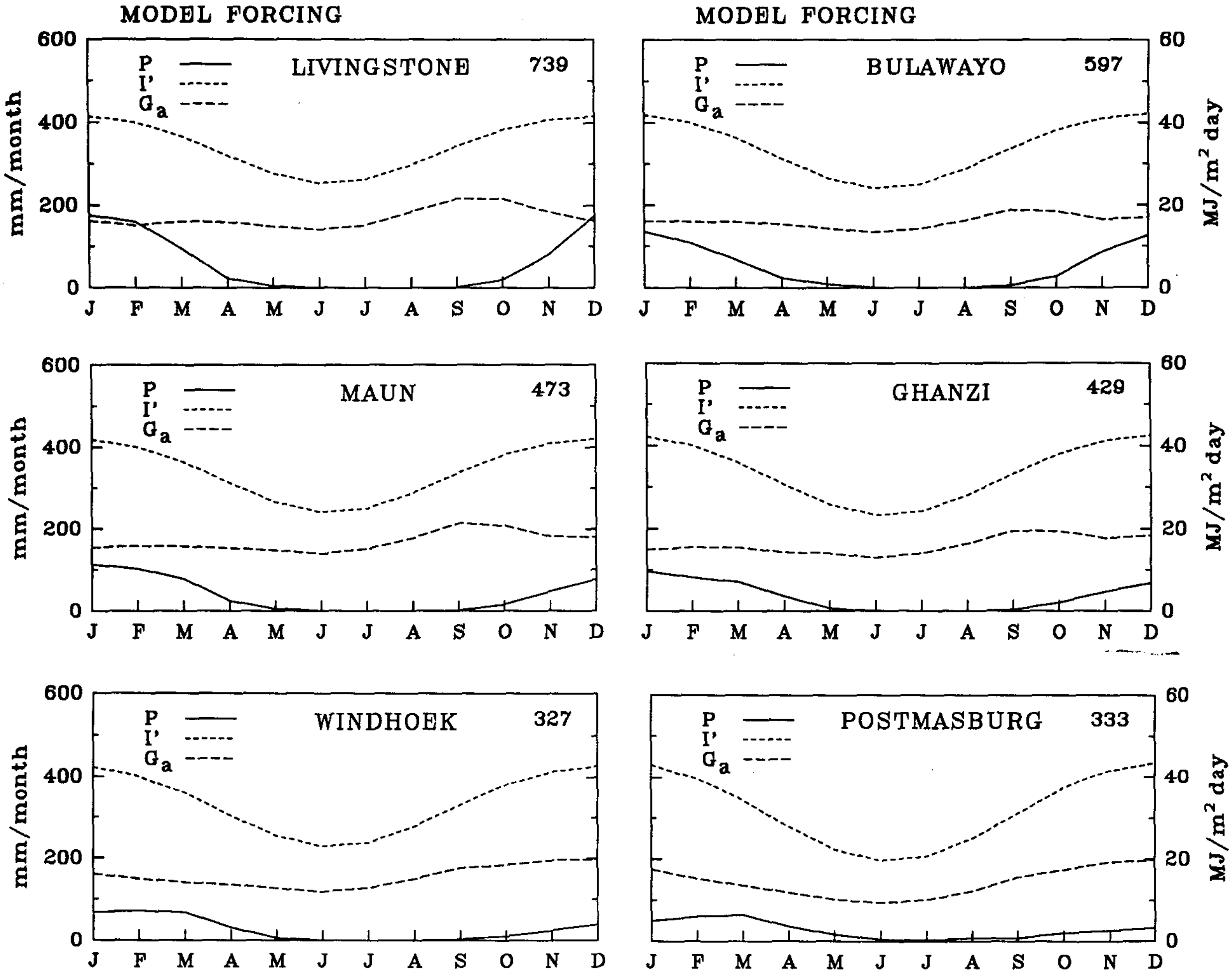

FIG. 4. (*Continued*)

TABLE 2. Parameters necessary for model input, as well as source used in study.

Parameter	Source
Shortwave radiation submodel	
Surface albedo	Dorman and Sellers (1989)
Cloud cover	Warren et al. (1986)
Rayleigh scattering	Bird and Hulstrom (1981)
Optical air mass	Rodgers (1967)
H_2O_V	Lacis and Hansen (1974); FAO (1984)
CO_2	Sasamori et al. (1972)
O_2	Sasamori et al. (1972)
O_3	Lacis and Hansen (1974); London et al. (1976)
Evapoclimatonomy submodel	
Vegtation cover	Dorman and Sellers (1989)
Soil texture	FAO/UNESCO (1977)
PET	FAO (1984)
Evaporivity (e*)	Lettau (1971); Pinker and Corio (1987); Nicholson and Lare (1990)

The precipitation difference between wet and dry years in the Kalahari (Fig. 6b) is roughly comparable to that of the Sahel both in magnitude and in size of the affected area. Important contrasts are evident in the difference fields for other hydrologic variables, however. In most of the area, the difference in soil moisture between wet and dry years is less than 10 mm, and the difference in ET seldom exceeds 30 mm mo^{-1}. Furthermore, the change of latitudinal gradients that are apparent over the Sahel are not apparent over the Kalahari. Also, the wet–dry contrast in runoff exceeds 50 mm mo^{-1} in only a few locations.

An interesting feature occurs, in particular, over the northern Kalahari region, with respect to the water balance. Although the region has significantly higher rainfall in wet years compared to dry years (on the order of 50 to 100 mm mo^{-1}), evapotranspiration rates are lower in wet years than in dry years. This is primarily due to a larger percentage of rainfall in wet years

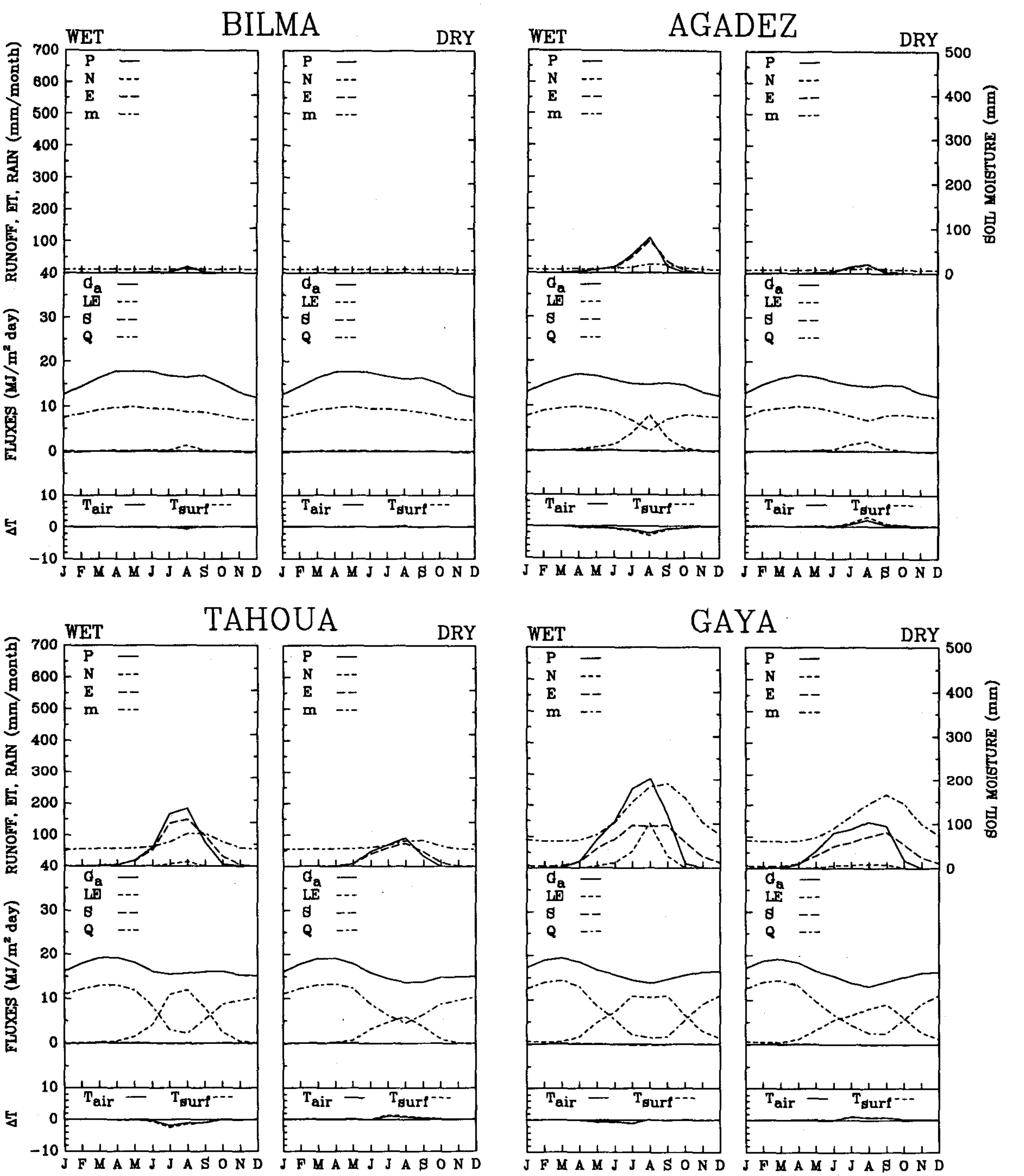

FIG. 5. Model results for the ten wettest years and ten driest years: P = precipitation, N = runoff, E = evapotranspiration, m = soil moisture. (a) Nine West African stations. (b) Six stations in or near the Kalahari.

being lost as immediate runoff, a direct manifestation of equation (20) if monthly mean infiltration rates are fairly low.

Overall, the contrast between the Kalahari and Sahel is probably primarily a result of timing, duration, and intensity of the rainy season. The season is longer, and of lower peak intensity in the Kalahari, and it occurs, unlike in the Sahel, when absorbed solar radiation is at a maximum. The magnitude and spatial coherence of the rainfall anomalies also differ to some extent in the two regions, however.

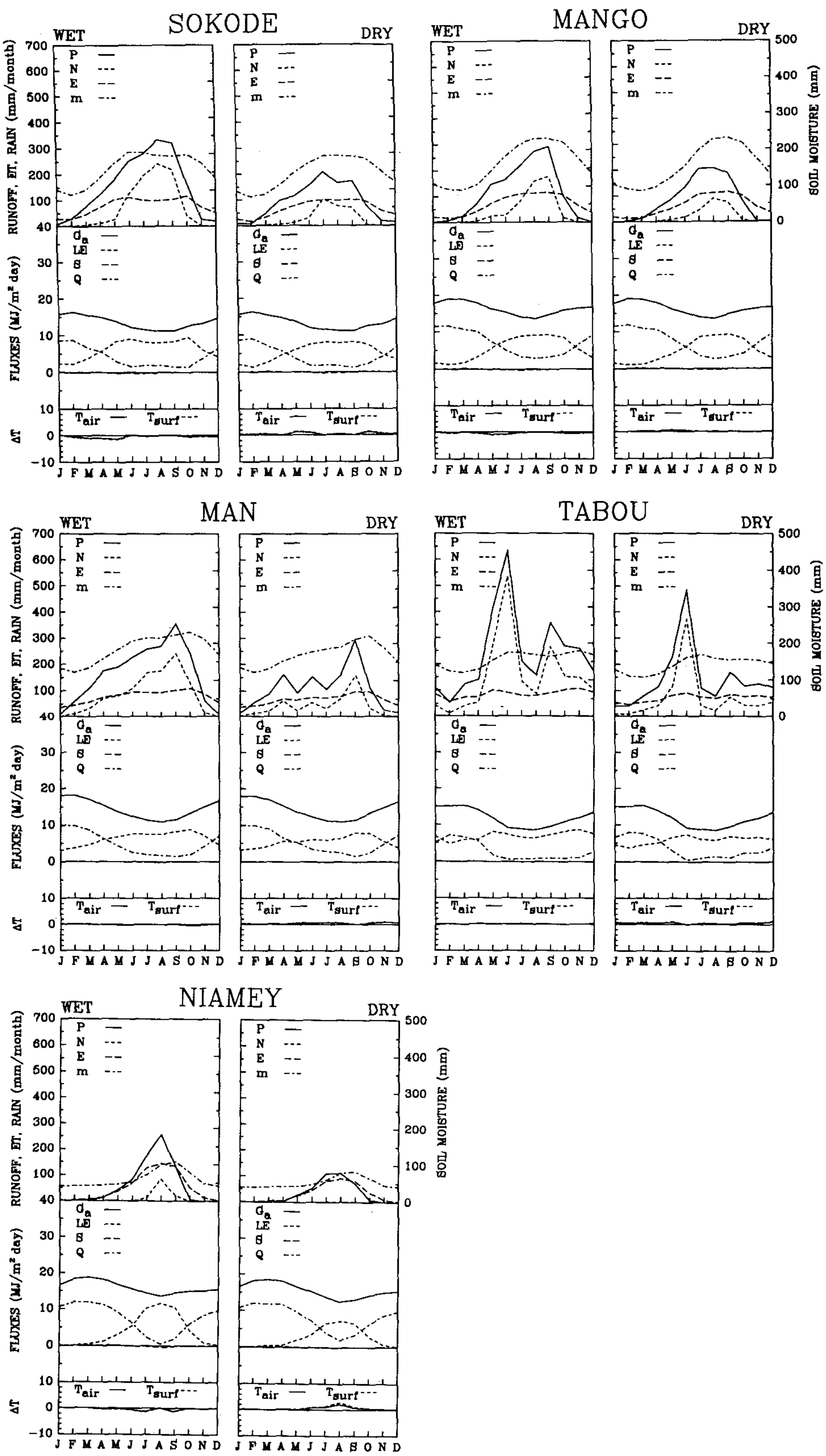

FIG. 5. (*Continued*)

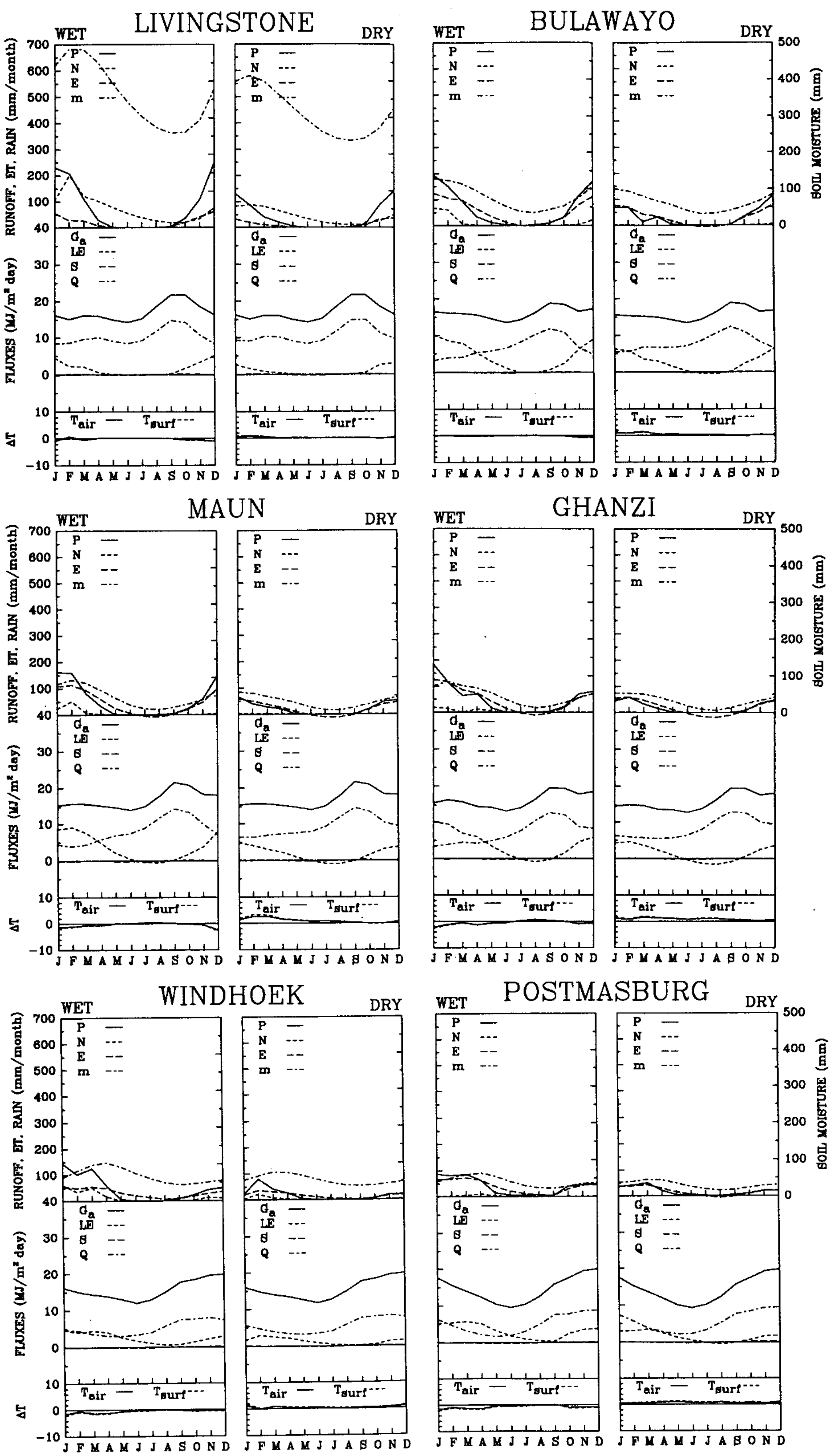

FIG. 5. (*Continued*)

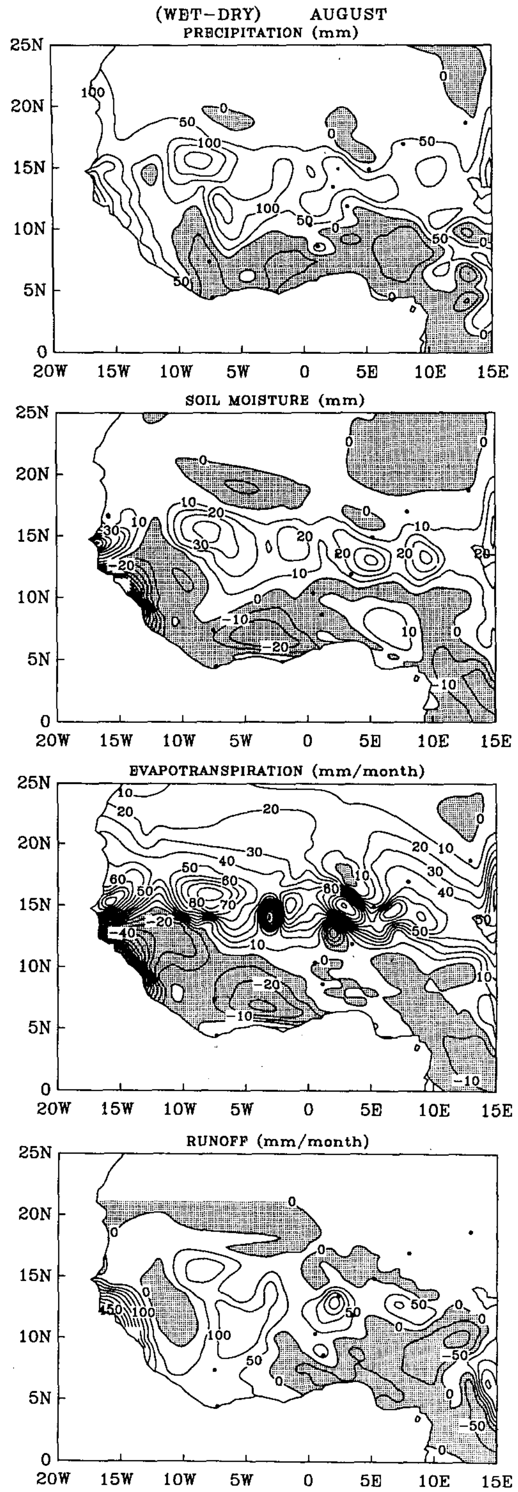

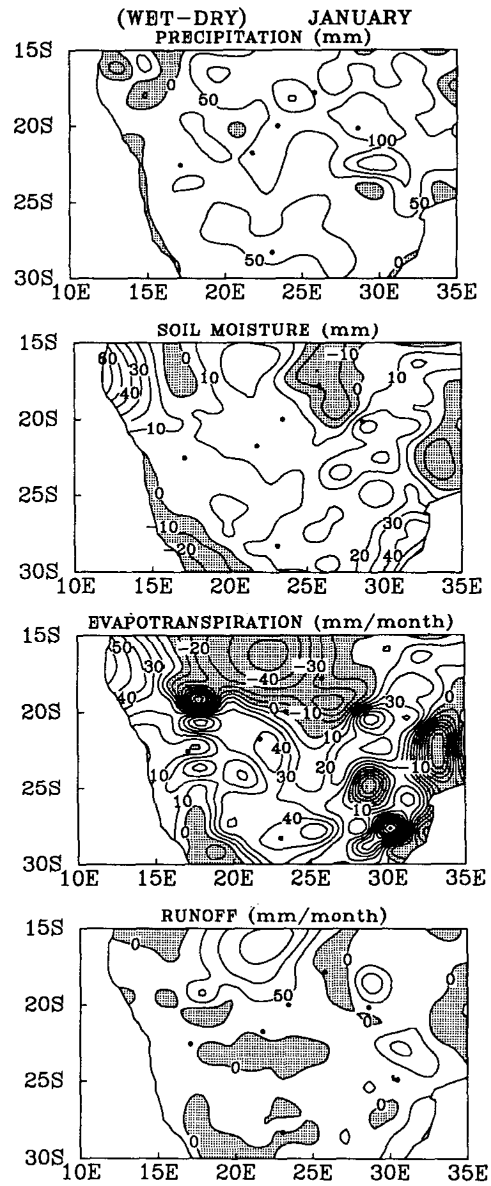

FIG. 6. (a) Differences in August precipitation, evapotranspiration, soil moisture and runoff between the ten wettest and ten driest years for the Sahel as a whole. (b) Differences in January precipitation, evapotranspiration, soil moisture, and runoff between the ten wettest and ten driest years for the Kalahari as a whole (contours are 50 mm mo^{-1} for precipitation and runoff, 10 mm mo^{-1} for ET, and 10 mm for soil moisture; shading indicates negative values).

c. Meridional gradients of latent heat in West Africa between wet and dry years and their consequences

West Africa is somewhat unique in that the dynamical system most closely linked to rain-bearing disturbances, the African easterly jet (AEJ), is a direct manifestation of land surface processes. This jet, essentially an easterly wind maximum of about 10 m s^{-1}, with its core in the midtroposphere at about 650 to 700 mb, is a consequence of the temperature gradient between the Sahara desert and the cooler Guinea Coast and Atlantic Ocean to the south. The AEJ is strongest at about 15°N.

The jet provides the energy and instability for the development, maintenance, and propagation of the rain-producing disturbances in the region. Cloud clusters produce about 90% of the rainfall in the Sahel; their frequency and the amount of rainfall they produce is modulated by transient easterly waves (Houze and Betts 1981). The westward-propagating waves originate as a consequence of the joint baroclinic–barotropic instability associated with the horizontal and vertical shear of the AEJ (Burpee 1972; Albignat and Reed 1980), and they are therefore confined to a relatively narrow latitudinal zone near and south of the jet core. There are consistent changes in intensity and shear of the jet between wet and dry years, with the jet (and shear) being stronger during dry years (Newell and Kidson 1984). Since the difference between an abnormally wet or dry rainy season month can be accounted for by as few as one or two intense disturbances, and the most intense systems are associated with easterly waves produced from the AEJ, the character of the rainy system is very sensitive to fluctuations in the jet. As the relevant jet shears and intensity are a function of the north–south temperature gradient in the region, the jet should be modulated by land surface fluxes such as latent heat. Thus, any land surface changes that are induced by anomalous wet or dry conditions should affect the surface radiation balance, and thereby, the AEJ. This in turn may result in the hypothesized positive feedback effect, and thus, enhance or prolong existing wet or dry conditions.

We have examined the latitudinal gradient of latent heating in wet and dry years along the transect shown in Fig. 3, using the nine Sahelian stations. The contrast between wet years and dry years is strong enough to affect the speed of the jet (Fig. 7). In the wet years, the latent heat flux to the atmosphere has a maximum at about 12°N to 13°N in July and September, and at about 15°N in August. The largest contrast between wet and dry years is apparent in August. In dry years, the maximum latent heating is at 10°N to 11°N in all months and there is little difference between wet and dry years from there southward. Latitudinally, the wet/dry contrast is largest at about 15°N in August and at about 12° or 13°N to 16°N in July and September. The flux of heat in these latitudes is about 4 to 6 MJ m^{-2} day^{-1} larger in wet years than in dry years.

It is difficult to assess the effect on the jet without a detailed model of atmospheric heating. Moreover, the differences in latent heat flux can act as a feedback mechanism producing interannual persistence only if it can be demonstrated that the heating anomaly persists until the following rainy season. Nevertheless, a rough estimate can be made of the effect on the jet's core speed and shear by considering the thermal wind equation and making certain assumptions about atmospheric heating.

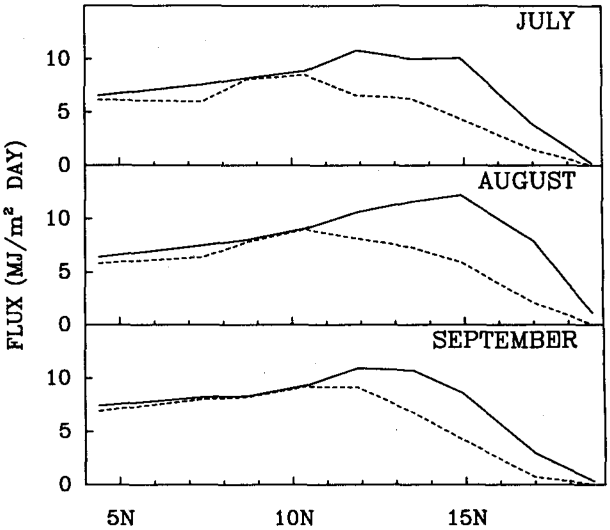

FIG. 7. Surface flux of latent heat as a function of latitude in July, August, and September in the ten wettest (solid) and ten driest (dashed) years in the West African Sahel.

The jet is a consequence of the temperature gradient, the relevant thermal wind speed U being computed according to

$$U = \frac{-R}{f}\left(\frac{\partial \bar{T}}{\partial y}\right)_p \ln\left(\frac{P_0}{P_1}\right), \tag{25}$$

where $(\partial \bar{T}/\partial y)_p$ is the mean latitudinal temperature gradient in the layer between pressure levels P_0 and P_1, R is the gas constant for dry air, and f is the Coriolis force. As the midtropospheric temperatures are higher to the north (i.e., over the Sahara) than to the south, the thermal wind (and the jet) is easterly.

Using the climatonomy output of surface temperature, two-meter air temperature, latent heat flux, and sensible heat flux, mean temperature profiles are derived for nine latitudinal bands, each corresponding to one of the base stations along the transect in Fig. 3. Appropriate means are derived for the bands using additional stations as described in section 2d. Calculations are made only for August. From the surface to the top of the surface layer (assumed to be 1/10 the height from the surface to the lifting condensation level), sensible heat flux is used to determine atmospheric temperature, as in Lettau and Lettau (1975). From the top of the surface layer to the lifting condensation level, that is, the mixed layer, a dry-adiabatic lapse rate is assumed. Once the lifting condensation level is reached, the temperature profile is assumed to follow a pseudoadiabat, which is determined using moist static energy, an approximately conserved quantity during a convective process. For simplicity, no entrainment zone or upper-level inversions are incorporated. Inherent in the surface temperatures for wet and dry years are implicit differences in saturation specific humidity and in the level at which condensation begins to occur. In other words, the moist static energy differs between wet and dry years.

Since the gradient of latent heating from south to north (about 12° or 13°N to 18°N) is the inverse of the temperature gradient, the sharper gradient during wet years acts to reduce the temperature gradient, thereby weakening the jet and jet shear in wet years. This is consistent with the weaker jet and jet shear observed by Newell and Kidson (1984) in wet years.

Taking a linear least-squares fit of the temperatures at the 700-mb level for the nine latitudinal bands centered at 15°N, as calculated above, corresponding geostrophic winds are calculated with the aid of Eq. (25). The calculations indicate a weakening of the African easterly jet on the order of 2.6 m s^{-1} between dry and wet years. That shown by Newell and Kidson (1984) is about 2 m s^{-1}. At 10°N, Newell and Kidson show a decrease of over 4 m s^{-1}. Our results show a decrease approximately twice that amount. At this latitude, however, the Coriolis force is very small and the thermal wind calculations are therefore highly sensitive to the north–south temperature gradient. Any slight discrepancy in the temperature gradient between that calculated and that observed will have a dramatic effect on the magnitude of the thermal wind speeds. A more detailed discussion of the effects of differences between wet and dry years on latent heating and on the African easterly jet will appear in a later article.

5. Summary and conclusions

The Lettau climatonomy model was used to examine the temporal and spatial effects of the Sahelian drought on land surface feedback. This was compared with the Sahelian Southern Hemisphere counterpart, the Kalahari, a region subject to similar large-scale atmospheric forcing, but lacking the Sahel's decadal persistence in rainfall anomalies. The effect of surface energy flux modification upon the midtropospheric winds, in particular the African easterly jet (AEJ), over West Africa was also explored. It is known that the AEJ is responsible for the development and maintenance of the West African disturbance lines, which bring most of the precipitation to West Africa.

These model results indicate that there are significant differences in the surface water balance between dry and wet years. The changes in the Sahel are more intensive, larger in spatial scale, and more spatially coherent than those in the Kalahari. Thus, the possibility of land surface–atmosphere feedback is higher in the Sahel than in the Kalahari. In drier regions, increased rainfall is manifested as higher soil moisture and ET. In wetter regions, it is manifested primarily as increased runoff.

South of the Sahara, this tends to decrease the surface gradient of latent heat exchange with the atmosphere during wet years. Consequently, the temperature gradient in the midtroposphere, where the latent heat is released, is also reduced. This in turn reduces the thermal wind and the intensity of wind and wind shear in the African easterly jet. The calculated magnitudes of these changes are consistent with those observed by Newell and Kidson (1984) in a study contrasting wet and dry years in the Sahel.

The calculations were performed for the peak rainy season months. They suggest that the magnitude of the change in surface energy balance between a wet and dry year is large enough to significantly affect the general atmospheric circulation, and thereby, the rainbearing systems. However, for this to provide a feedback mechanism that can produce the characteristic interannual persistence of Sahelian rainfall anomalies, there must be a "memory" extending to the following rainy season. A more detailed atmospheric model is required to test this hypothesis.

Acknowledgments. We would like to thank Heinz Lettau for many valuable discussions of the climatonomy model. We would also like to acknowledge support from NASA Grants NAG 5-764 and NGT 50475 and from NSF Grant ATM 9024340.

REFERENCES

Albignat, J. P., and R. J. Reed, 1980: The origin of African wave disturbances during Phase III of GATE. *Mon. Wea. Rev.*, **108**, 1827–1839.

Bird, R., and R. L. Hulstrom, 1981: Review, evaluation, and improvement of direct irradiance models. *Trans. ASME J. Sol. Energy Eng.*, **103**, 182–192.

Burpee, R. W., 1972: The origin and structure of easterly waves in the lower troposphere of North Africa. *J. Atmos. Sci.*, **29**, 77–90.

Corio, L. A., and R. T. Pinker, 1987: Estimating monthly mean water and energy budgets over the central U.S. Great Plains. Part II. Evapoclimatonomy experiments. *Mon. Wea. Rev.*, **115**, 1153–1160.

Dorman, J. L., and P. J. Sellers, 1989: A global climatology of albedo, roughness length, and stomatal resistance for atmospheric general circulation models as represented by the simple biosphere model (SiB). *J. Appl. Meteor.*, **28**, 833–855.

Eagleson, P. S., and R. I. Segarra, 1985: Water-limited equilibrium of savanna vegetation systems. *Water Resour. Res.*, **21**, 1483–1493.

——, N. M. Fennessey, Q. Wang, and I. Rodriquez-Iturbe, 1987: Application of spatial Poisson models to air mass thunderstorm rainfall. *J. Geophys. Res.*, **92**, 9661–9678.

FAO, 1984: *Agroclimatological Data, Vol. I and II*, Food and Agricultural Organization.

FAO/UNESCO, 1977: *Soil Map of the World. Vol. VI, Africa.* UNESCO, 218 pp.

Gifford, G. F., 1984: Vegetation allocation for meeting site requirement. *Development Strategies for Rangeland Management.* Westview Press, 35–116.

Houze, R. A., Jr., and A. K. Betts, 1981: Convection in GATE. *Rev. Geophys. Space Phys.*, **19**, 541–576.

Lacis, A. A., and J. E. Hansen, 1974: A parameterization for the absorption of solar radiation in the earth's atmosphere. *J. Atmos. Sci.*, **31**, 118–133.

Lare, A. R., and S. E. Nicholson, 1990: A climatonomic description of the surface energy balance in the Central Sahel. Part I: Shortwave radiation. *J. Appl. Meteor.*, **29**, 123–137.

Lettau, H. H., 1969: Evapotranspiration climatonomy. I. A new approach to numerical prediction of monthly evapotranspiration, runoff, and soil moisture storage. *Mon. Wea. Rev.*, **97**, 691–699.

——, and K. Lettau, 1969: Shortwave radiation climatonomy. *Tellus*, **21**, 208–222.

——, and M. W. Baradas, 1973: Evapotranspiration climatonomy. II: Refinement of parameterization, exemplified by application to the Macaban River watershed. *Mon. Wea. Rev.*, **101**, 636–649.

——, and ——, 1975: Regional climatonomy of tundra and boreal forests in Canada. Climate of the Arctic. *Proc. 24th Alaskan Science Conference*, Fairbanks, AAAS and Amer. Meteor. Soc., 209–221.

——, and E. J. Hopkins, 1991: Evapoclimatonomy III: The reconcilitation of monthly runoff and evaporation in the climatic balance of evaporable water on land areas. *J. Appl. Meteor.*, **30**, 776–792.

Lettau, K., 1971: Radiation climate of New Delhi. Part II: Longwave radiation and energy budget. *Indian J. Meteor. Geophys.*, **22**, 529–540.

London, J., R. D. Bojkov, S. Oltmans, and J. E. Kelley, 1976: Atlas of the Global Distribution of Total Ozone, July 1957–June 1967. Report No. NCAR/TN-113+STR, National Science Foundation, 276 pp. [NTIS PB258882.]

Milly, P. C. D., and P. S. Eagleson, 1982: Parameterization of moisture and heat fluxes across the land surface for use in atmospheric general circulation models. Report No. 279, M.I.T., 226 pp. [Available from Ralph M. Parsons Laboratory, Cambridge, MA 02139.]

Mintz, Y., and Y. Serafini, 1984: Global fields of monthly normal soil moisture, as derived from observed precipitation and an estimated potential evapotranspiration. Final scientific report under NASA Grant No. NAS 5-26, part V. Department of Meteorology, University of Maryland. [Available from Department of Meteorology, University of Maryland, College Park, MD 20742.]

Newell, R. E., and J. W. Kidson, 1984: African mean wind changes between Sahelian wet and dry periods. *J. Climatol.*, **4**, 27–33.

Nicholson, S. E., 1986: The spatial coherence of African rainfall anomalies: Interhemispheric teleconnections. *J. Climate Appl. Meteor.*, **25**, 1365–1381.

——, and A. R. Lare, 1990: A climatonomic description of the surface energy balance in the central Sahel. Part II: The evapoclimatonomy submodel. *J. Appl. Meteor.*, **29**, 138–146.

Pinker, R. T., and L. A. Corio, 1987: Estimating monthly mean water and energy budgets over the central U.S. Great Plains. Part I: Evapoclimatonomy model formulation. *Mon. Wea. Rev.*, **115**, 1140–1152.

Rawls, W. J., and D. L. Brakensiek, 1989: Estimation of soil water retention and hydraulic properties. *Unsaturated Flow in Hydrologic Modeling: Theory and Practice.* H. J. Morel-Seytoux, Ed. Kluwer Academic Publishers, 275–300.

——, ——, and M. R. Savabi, 1989: Infiltration parameters for rangeland soils. *J. Range Manag.*, **42**, 139–142.

Rodgers, C. D., 1967: The radiative heat budget of the troposphere and lower stratosphere. Rep. No. A2, Planetary Circulation Project, Department of Meteorology, M.I.T., 99 pp. [NTIS PB176-527.]

Sasamori, T., J. London, and D. V. Hoyt, 1972: Radiation budget of the Southern Hemisphere. *Meteorology of the Southern Hemisphere, Meteor. Monogr.*, No. 13, Amer. Meteor. Soc., 9–23.

Saxton, K. E., W. J. Rawls, J. S. Romberger, and R. J. Papendick, 1986: Estimating generalized soil-water characteristics from texture. *Soil Sci. Soc. Amer. J.*, **50**, 1031–1036.

Sellers, W. D., 1965: *Physical Climatology.* The University of Chicago Press, 272 pp.

Serafini, Y. V., and Y. C. Sud, 1987: The time scale of the soil hydrology using a simple water budget model. *J. Climatol.*, **7**, 585–591.

Spencer, J. W., 1971: Fourier series representation of the position of the sun. *Search*, **2**, 172.

Trewartha, G. T., 1961: *The Earth's Problem Climates.* The University of Wisconsin Press, 334 pp.

Warren, S. G., C. J. Hahn, J. London, R. M. Chervin, and R. L. Jenne, 1986: Global distribution of total cloud cover and cloud type amounts over land. NCAR/TN-273+STR, 230 pp. [NTIS PR-360.]

Warrilow, D. A., 1986: The sensitivity of the U.K. Meteorological Office atmospheric general circulation model to recent changes to the parameterization of hydrology. *Proc. International Satellite Land-Surface Climatology Project Conference, Rome, Italy*, ESA SP-248, 143–149.

Wilcox, B. P., W. J. Rawls, D. L. Brakensiek, and J. R. Wight, 1990: Predicting runoff from rangeland catchments: A comparison of two models. *Water Resour. Res.*, **26**, 2401–2410.